Polarization rotation vector solitons in a graphene mode-locked fiber laser

Song, Yu Feng; Zhang, Han; Tang, Dingyuan; Shen, De Yuan

2012

Song, Y. F., Zhang, H., Tang, D., & Shen, D. Y. (2012). Polarization rotation vector solitons in a graphene mode-locked fiber laser. Optics express, 20(24), 27283-27289.

https://hdl.handle.net/10356/99900

https://doi.org/10.1364/OE.20.027283

Polarization rotation vector solitons in a graphene mode-locked fiber laser

Yu Feng Song,[1] Han Zhang,[1] Ding Yuan Tang,[1,*] and De Yuan Shen[2]

[1]*School of Electrical and Electronic Engineering, Nanyang Technological University, Singapore*
[2]*School of Physics and Electronic Engineering, Jiangsu Normal University, 221116 China*
[*]*edytang@ntu.edu.sg*

Abstract: Polarization rotation vector solitons formed in a fiber laser passively mode locked with atomic layer graphene were experimentally investigated. It was found that different from the case of the polarization locked vector soliton formed in the laser, two extra sets of spectral sidebands always appear on the soliton spectrum of the polarization rotating vector solitons. We confirm that the new sets of spectral sidebands have the same formation mechanism as that of the Kelly sidebands.

OCIS codes: (060.4370) Nonlinear optics, fibers; (060.5530) Pulse propagation and temporal solitons.

References and links

1. C. R. Menyuk, "Stability of solitons in birefringent optical fibers. I: Equal propagation amplitudes," Opt. Lett. **12**(8), 614–616 (1987).
2. V. V. Afanasjev, "Soliton polarization rotation in fiber lasers," Opt. Lett. **20**(3), 270–272 (1995).
3. D. N. Christodoulides and R. I. Joseph, "Vector solitons in birefringent nonlinear dispersive media," Opt. Lett. **13**(1), 53–55 (1988).
4. N. Akhmediev, A. Buryak, and J. M. Soto-Crespo, "Elliptically polarised solitons in birefringent optical fibers," Opt. Commun. **112**(5-6), 278–282 (1994).
5. M. N. Islam, C. D. Poole, and J. P. Gordon, "Soliton trapping in birefringent optical fibers," Opt. Lett. **14**(18), 1011–1013 (1989).
6. S. T. Cundiff, B. C. Collings, and W. H. Knox, "Polarization locking in an isotropic, modelocked soliton Er/Yb fiber laser," Opt. Express **1**(1), 12–21 (1997).
7. L. M. Zhao, D. Y. Tang, H. Zhang, and X. Wu, "Polarization rotation locking of vector solitons in a fiber ring laser," Opt. Express **16**(14), 10053–10058 (2008).
8. L. M. Zhao, D. Y. Tang, X. Wu, H. Zhang, and H. Y. Tam, "Coexistence of polarization-locked and polarization-rotating vector solitons in a fiber laser with SESAM," Opt. Lett. **34**(20), 3059–3061 (2009).
9. J. H. Wong, K. Wu, H. H. Liu, C. Ouyang, H. Wang, S. Aditya, P. Shum, S. Fu, E. J. R. Kelleher, A. Chernov, and E. D. Obraztsova, "Vector solitons in a laser passively mode-locked by single-wall carbon nanotubes," Opt. Commun. **284**(7), 2007–2011 (2011).
10. R. Gumenyuk, M. S. Gaponenko, K. V. Yumashev, A. A. Onushchenko, and O. G. Okhotnikov, "Vector soliton bunching in thulium-holmium fiber laser mode locked with PbS quantum-dot-doped glass absorber," IEEE J. Quantum Electron. **48**(7), 903–907 (2012).
11. X. Wu, D. Y. Tang, L. M. Zhao, and H. Zhang, "Mode-Locking of fiber lasers induced by residual polarization dependent loss of cavity components," Laser Phys. **20**(10), 1913–1917 (2010).
12. Q. Bao, H. Zhang, Y. Wang, Z. Ni, Y. Yan, Z. X. Shen, K. P. Loh, and D. Y. Tang, "Atomic-layer graphene as a saturable absorber for ultrafast pulsed lasers," Adv. Funct. Mater. **19**(19), 3077–3083 (2009).
13. H. Zhang, D. Y. Tang, L. M. Zhao, Q. L. Bao, and K. P. Loh, "Vector dissipative solitons in graphene mode locked fiber lasers," Opt. Commun. **283**(17), 3334–3338 (2010).
14. W. D. Tan, C. Y. Su, R. J. Knize, G. Q. Xie, L. J. Li, and D. Y. Tang, "Mode locking of ceramic Nd:yttrium aluminum garnet with graphene as a saturable absorber," Appl. Phys. Lett. **96**(3), 031106 (2010).
15. J. Ma, G. Q. Xie, P. Lv, W. L. Gao, P. Yuan, L. J. Qian, H. H. Yu, H. J. Zhang, J. Y. Wang, and D. Y. Tang, "Graphene mode-locked femtosecond laser at 2 μm wavelength," Opt. Lett. **37**(11), 2085–2087 (2012).
16. S. M. J. Kelly, "Characteristic sideband instability of periodically amplified average soliton," Electron. Lett. **28**(8), 806–807 (1992).
17. H. Zhang, D. Y. Tang, L. M. Zhao, and N. Xiang, "Coherent energy exchange between components of a vector soliton in fiber lasers," Opt. Express **16**(17), 12618–12623 (2008).
18. S. Trillo, S. Wabnitz, R. H. Stolen, G. Assanto, C. T. Seaton, and G. I. Stegeman, "Experimental observation of polarization instability in a birefringent optical fiber," Appl. Phys. Lett. **49**(19), 1224–1226 (1986).
19. K. J. Blow, N. J. Doran, and D. Wood, "Polarization instabilities for solitons in birefringent fibers," Opt. Lett. **12**(3), 202–204 (1987).

#173586 - $15.00 USD Received 1 Aug 2012; revised 3 Sep 2012; accepted 4 Sep 2012; published 19 Nov 2012

20. M. Haelterman, S. Trillo, and S. Wabnitz, "Dissipative modulation instability in a nonlinear dispersive ring cavity," Opt. Commun. **91**(5-6), 401–407 (1992).

1. Introduction

Vector soliton formation in birefringent single mode fibers (SMFs) was theoretically extensively investigated in the past. C. R. Menyuk first theoretically studied optical pulse propagation in birefringent optical fibers [1]. He found that above a certain pulse intensity level two orthogonally polarized solitons with different centre wavelengths could couple together and propagate at the same group velocity. The entity of the coupled solitons was later known as a group velocity locked vector soliton. V. V. Afanasjev theoretically investigated the pulse propagation in weakly birefringent SMFs and found an approximate analytic solution for the polarization rotation vector soliton [2]. Christodoulides and Joseph [3], and Akhmediev et al. [4] theoretically predicted different forms of polarization locked vector solitons in weakly birefringent optical fibers. In contrast to the theoretical studies, except that the group velocity locked vector soliton was experimentally confirmed [5], experimental observations on the other types of the theoretically predicted vector solitons were hampered by the stringent requirement on the birefringence property of the SMFs. To form these types of vector solitons the SMFs need to have stable weak birefringence over a long distance, while in practice it is difficult to make such SMFs. However, it was recently found that the requirement could be leveraged if the optical pulse is propagating in a fiber cavity, where as far as the average birefringence over one cavity roundtrip is close to zero, the phase locked vector solitons could be formed. Using the technique S. T. Cundiff et al. first experimentally observed vector solitons in a passively mode locked fiber laser [6]. In their experiment both the polarization rotating and the polarization locked vector solitons were obtained. Vector soliton formation in passively mode locked fiber lasers were also experimentally confirmed by several other groups [7–10].

A crucial condition for the vector soliton formation in fiber lasers is that no any polarization discrimination components should be used in the cavity. It has been demonstrated experimentally that even inserting a component with about 30% polarization discrimination could cause the nonlinear polarization rotation (NPR) mode locking of a fiber laser that is made of all anomalous dispersion fibers [11]. The existence of a polarization discrimination component in cavity will fix the polarization of light at the cavity position. Under effect of the cavity boundary condition the polarization of light is then fixed everywhere in the cavity. No intrinsic polarization dynamics of the vector solitons could be obtained in the fiber lasers.

In a previous paper we reported the vector soliton operation of a fiber laser mode-locked with the atomic-layer graphene [12]. Graphene is a single two-dimensional atomic layer of carbon atoms arranged in a honeycomb structure. It has been shown that graphene possesses not only extraordinary electronic properties but also novel optical properties. An example of its novel optical property is its broadband saturable absorption, which has been exploited for passively mode locking lasers of different wavelengths [13–15]. The two dimensional structure of graphene determines that its saturable absorption is independent of the light polarization when the light is incident perpendicularly to its plane. Like a semiconductor saturable absorption mirror (SESAM), this polarization insensitive saturable absorption of graphene could be used to passively mode lock a laser and introduce no polarization discrimination. As graphene saturable absorbers are easy to make, and have superbroad bandwidth and variable modulation depth when different number of graphene layers is used, it is superior for generating vector solitons in fiber lasers. In this paper we further report on features of the vector solitons formed in a graphene mode locked erbium fiber laser.

#173586 - $15.00 USD Received 1 Aug 2012; revised 3 Sep 2012; accepted 4 Sep 2012; published 19 Nov 2012

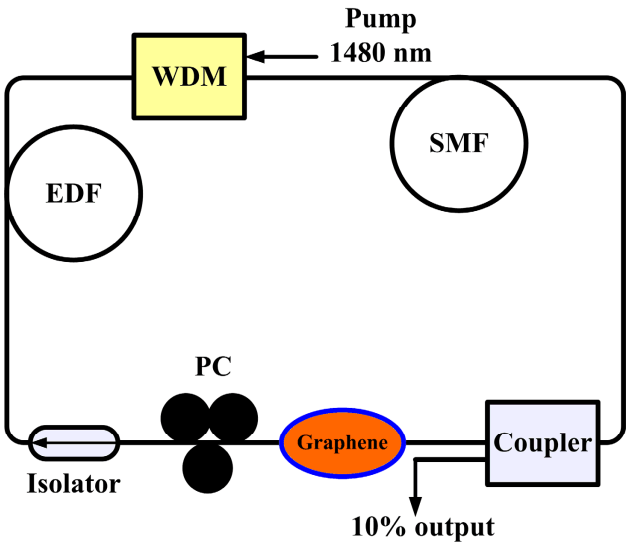

Fig. 1. A schematic of the experimental setup. PC: Polarization controller, EDF: Erbium doped fiber, SMF: Single-mode fiber, WDM: Wavelength-division multiplexer.

2. Experimental setup and results

The graphene mode-locked fiber laser is schematically shown in Fig. 1. The laser cavity is a ring that consists of 0.7 m erbium-doped fiber (EDF Er80-8/125 from Liekki) with group velocity dispersion (GVD) of –22 fs^2/mm and 22 m standard SMF. In addition, a 10% fiber output coupler was used to output the signal, a polarization independent isolator was used to force the unidirectional operation of the ring cavity, and an intra-cavity polarization controller (PC) was used to fine tune the linear cavity birefringence. All these passive components are made of the SMF or pigtailed with SMFs. The laser was pumped by a high power Raman fiber laser (KPS-BT2-RFL-1480-60-FA) of wavelength 1480 nm. The graphene was fabricated with the chemical vapour deposition method [12] and the graphene sheets were deposited on a standard FC/PC fiber connector. It is estimated that the graphene used have 3~5 atomic layers with a saturable absorption modulation depth of ~23%. The soliton spectra of the laser were measured with an optical spectrum analyzer (ANDO AQ6317). A 1 GHz oscilloscope (Lecroy Waverunner 6100) together with three 2 GHz photo-detectors (Thorlab DET01CFC) was used to monitor the soliton pulse train emitted by the laser.

#173586 - $15.00 USD Received 1 Aug 2012; revised 3 Sep 2012; accepted 4 Sep 2012; published 19 Nov 2012

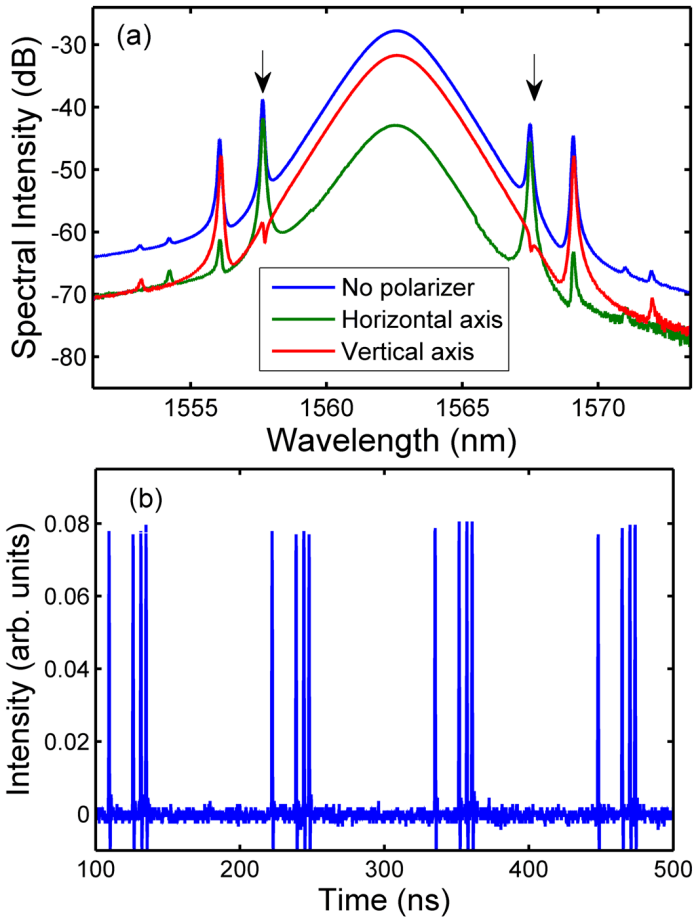

Fig. 2. Vector soliton emission of the fiber laser. (a) Soliton spectra. Blue line: the total laser emission without passing through a polarizer; Red and Green lines: the two orthogonal polarization components resolved with an external cavity polarization beam splitter. (b) Oscilloscope trace of the solitons.

Self-started mode locking is always obtained in the laser when the pump power is increased to ~90 mW. Immediately after mode locking, multiple pulses are normally obtained in the laser cavity. Occasionally the pulses are observed moving randomly in the cavity. However, through carefully adjusting the intracavity polarization controller and/or changing the pump power, a stable state where the multiple pulses stay stationary with respect to each other in the cavity, could be obtained. Figure 2 shows for example such a state. Figure 2(a) is the measured optical spectrum. Kelly sidebands are obvious on the spectrum [16], confirming that the pulses are optical solitons. The central wavelength of the solitons is at 1562.40 nm. Figure 2(b) is the measured oscilloscope trace of the soliton pulses. In the state all the pulses in cavity have exactly the same pulse height, indicating that the solitons possess the soliton energy quantization property. We note that different from the soliton spectra obtained from a NPR mode locked fiber laser, apart from the Kelly sidebands, there are also another set of spectral sidebands (indicated by the arrows) on the soliton spectrum shown in Fig. 2(a). At first sight one may confuse that all the sharp spectral peaks on the soliton spectrum are the Kelly sidebands. However, as one carefully adjusts the intra cavity PC, it will be observed that one set of the spectral sidebands shift their positions remarkably on the soliton spectrum, while the other set of spectral sidebands have almost no position change. The latter set of spectral sidebands is the Kelly sidebands. We point out that the appearance of the other set of spectral sidebands is a result of the vector soliton formation in the fiber laser. To clearly

#173586 - $15.00 USD Received 1 Aug 2012; revised 3 Sep 2012; accepted 4 Sep 2012; published 19 Nov 2012

identify the difference of the spectral sidebands, it is better to measure the polarization resolved spectra of the vector solitons. As in our laser there is no any polarization discrimination component in the cavity, the net cavity birefringence could be tuned to a very small value. Consequently, the formed solitons are all vector soliton and consist of two orthogonal polarization components. To simultaneously measure the polarization resolved spectra of the vector solitons, experimentally we used a fiber pigtailed external cavity polarization beam splitter to separate the two orthogonal polarization components. In order to balance the fiber pigtail induced linear polarization rotation, we inserted a polarization controller between the laser output port and the polarization beam splitter. The polarization resolved spectra of the solitons measured are shown in Fig. 2(a). On the polarization resolved spectra while the Kelly sidebands always exhibit as spectral peaks, the other set of spectral sidebands displays either as a spectral peak or a spectral dip, between the two orthogonal polarization components there always exists a peak-dip relationship, indicating the existence of coherent energy exchange between the two soliton components. In a previous paper we have shown that such spectral sidebands are formed due to the coherent coupling between the two polarization components of the vector solitons in a laser [17]. Here it is worth noting that four-wave mixing between the two orthogonal polarization components of light in weakly birefringent SMFs were experimentally observed by Trillo et al. [18] and numerically investigated by Blow et al. [19]. It was shown this effect could cause polarization instability. However, different from the case of light propagation in SMFs, which can be treated as a conservative system, light propagation in a laser cavity also experiences gain and losses. The formation of a stable soliton in a laser needs to fulfill the gain loss balance. Probably it is because of this difference no soliton polarization instability was observed in our experiment. Moreover, we note that a soliton circulating in a cavity also has to satisfy the cavity boundary condition. Haelterman et al. have theoretically shown that the cavity detuning could alter the phase matching condition of the coherent wave coupling in a dispersive cavity [20]. Indeed, in our experiments it was observed that the positions of the extra spectral sidebands vary remarkably with the adjustment of the paddles of the intra-cavity PC.

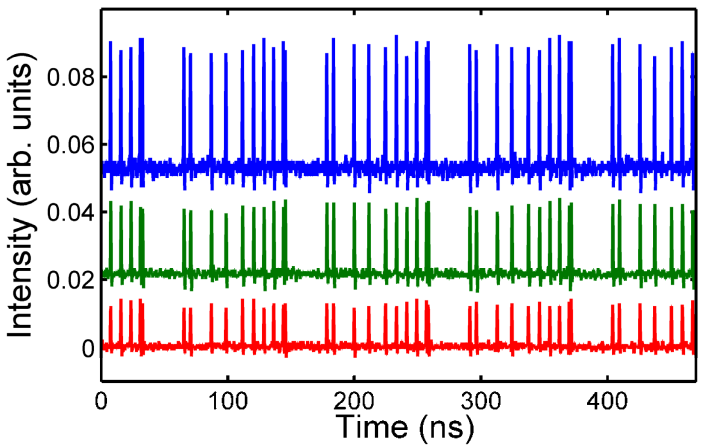

Fig. 3. Oscilloscope traces of the pulse train in a phase locked vector soliton operation state. Blue line: the total laser emission without passing through a polarizer; Red and Green lines: the two orthogonal polarization components resolved with an external cavity polarization beam splitter.

Like the appearance of Kelly sidebands is a characteristic of the soliton formation in a laser, we found that the appearance of the above extra spectral sidebands is a characteristic of the vector soliton formation in our fiber laser. Experimentally, we further noticed that depending on the laser operation conditions, two types of vector solitons could be formed. The polarization locked and polarization rotation ones. Figure 3 shows the oscilloscope traces of a state with multiple polarization locked vector solitons in cavity. In this case all vector

#173586 - $15.00 USD Received 1 Aug 2012; revised 3 Sep 2012; accepted 4 Sep 2012; published 19 Nov 2012

solitons in the cavity have exactly the same polarization and their polarization features remain unchanged as they propagate in the cavity. Therefore, when measured after an external cavity polarizer, after every cavity roundtrip all the solitons in the cavity remain the same pulse intensity. Optical spectra of all the polarization locked vector solitons are similar to those as shown in Fig. 2(a), except that the positions of the extra spectral sidebands vary.

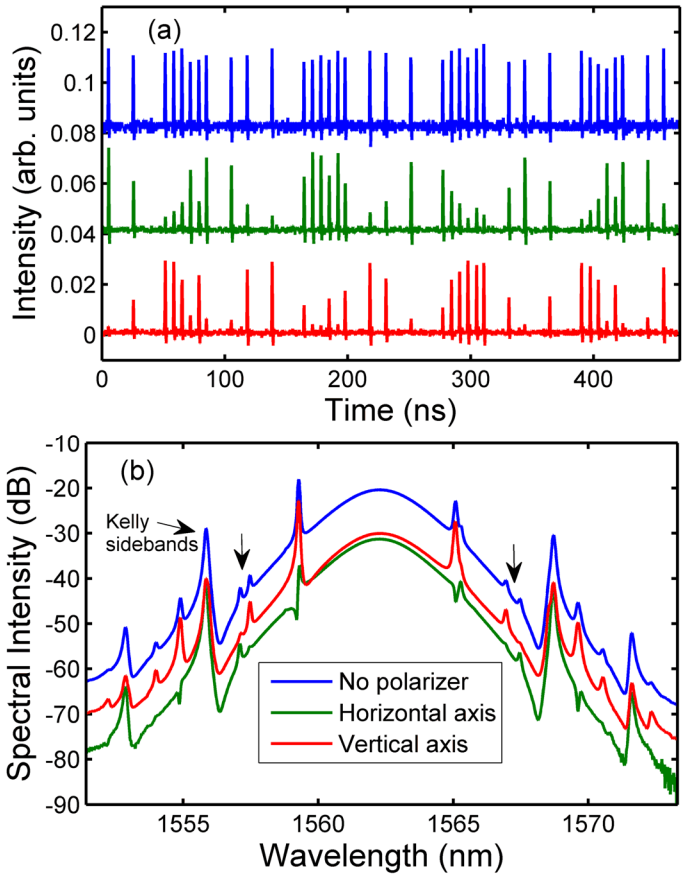

Fig. 4. A polarization rotation vector soliton state of the laser. (a) The total and the polarization resolved soliton pulse trains with multiple solitons in cavity. (b) Optical spectra of the solitons. Blue line: the total laser emission without passing through a polarizer; Red and Green lines: the two orthogonal polarization components resolved with an external cavity polarization beam splitter.

Figure 4 shows the oscilloscope traces and spectra of a polarization rotation vector soliton state. Without passing through an external cavity polarizer, the oscilloscope trace shows no difference to that of a polarization locked state, as shown in Fig. 3. However, from the polarization resolved traces, one can clearly identify the soliton pulse intensity variations. Carefully checking the pulse intensity variations, it can be identified that the polarization of the vector solitons shown in Fig. 4 is rotating in the cavity. After every three cavity-roundtrips their polarization rotated back. We found experimentally that whenever the polarization of the vector solitons was rotating in the cavity, another two sets of weak spectral sidebands (indicated with arrows in Fig. 4(b)) further appeared on the soliton spectrum. Comparing Fig. 4(b) with Fig. 2(a) it is to see that apart from the Kelly sidebands, there are another three sets of spectral sidebands visible on the soliton spectrum now. Based on the polarization resolved spectra, one set of the sidebands is due to the coherent energy exchange between the two orthogonal polarization components, as described above. Each of the other two sets of the weak new sidebands (indicated with arrows in Fig. 4(b)) appears only on

#173586 - $15.00 USD Received 1 Aug 2012; revised 3 Sep 2012; accepted 4 Sep 2012; published 19 Nov 2012

spectrum of one of the two orthogonal polarization components, respectively. Moreover, no matter how the two orthogonal polarization components are split, the weak new sidebands always exhibit as spectral peaks. No spectral dip could be obtained. The feature of the weak new sidebands is similar to that of the Kelly sidebands.

Obviously, the new sets of weak spectral sidebands are formed due to the polarization rotation of the vector solitons. The periodic polarization rotation of the vector solitons introduces an extra periodic soliton parameter variation, therefore, leads to the formation of another set of spectral sidebands. As the soliton polarization rotation has a different period than that of the soliton circulation in the cavity, the new spectral sidebands have different positions to those of the conventional Kelly sidebands. We point out that like the formation of the Kelly sidebands, the formation of the new weak spectral sidebands is a linear effect. They are caused by the constructive interference between the dispersive waves emitted by the solitons as their polarizations periodically rotate in the cavity. For a vector soliton it has two orthogonal polarization components, in a state of polarization rotation each soliton polarization component would have different phase. It could be due to the subtle difference between the two polarization components that each soliton component formed its own new spectral sidebands under polarization rotation of the vector solitons. Finally, we point out that although the polarization rotation spectral sidebands have the same formation mechanism as those of the Kelly sidebands, their positions varied remarkably with the laser operation conditions, because the rotation speed of the vector solitons varied with the experimental conditions.

3. Conclusions

In conclusion, we have experimentally investigated the vector soliton operation of a fiber laser mode locked with the atomic layer graphene. Both the polarization locked and polarization rotation vector solitons were observed in our laser. It was shown that the cavity effect always induces resonant energy exchange between the two orthogonal polarization components of the vector solitons. However, no polarization instability of the solitons was observed. For the polarization rotation vector solitons, it was found that two new sets of spectral sidebands would appear on the vector soliton spectrum, whose formation is due to the periodic polarization rotation of the vector solitons.

Acknowledgments

This project is supported by the AOARD under the contract number FA2386-11-4010. D. Y. Shen acknowledges support by the fund of Priority Academic Program Development of Jiangsu Higher Education Institutions (PAPD).

#173586 - $15.00 USD Received 1 Aug 2012; revised 3 Sep 2012; accepted 4 Sep 2012; published 19 Nov 2012